The Plant Journal (2012) doi: 10.1111/j.1365-313X.2012.05080.x

Quantitative levels of *Deficiens* and *Globosa* during late petal development show a complex transcriptional network topology of B function

María Manchado-Rojo, Luciana Delgado-Benarroch[†], María J. Roca[‡], Julia Weiss and Marcos Egea-Cortines[*]
Department of Genetics, ETSIA, Instituto de Biotecnología Vegetal, Universidad Politécnica de Cartagena, Paseo Alfonso XIII 48, 30203 Cartagena, Spain

Received 13 March 2012; revised 7 June 2012; accepted 11 June 2012.
*For correspondence (e-mail marcos.egea@upct.es).
[†]Present address: Instituto de Botánica del Nordeste (IBONE-CONICET), Facultad de Ciencias Agrarias, Universidad Nacional del Nordeste, Sargento Cabral 2131 CC 209, 3400 Corrientes, Argentina.
[‡]Present address: Servicio de Apoyo a la Investigación Tecnológica, Universidad Politécnica de Cartagena, Plaza del Hospital s/n, 30202 Cartagena, Spain.

SUMMARY

The transcriptional network topology of B function in *Antirrhinum*, required for petal and stamen development, is thought to rely on initial activation of transcription of *DEFICIENS* (*DEF*) and *GLOBOSA* (*GLO*), followed by a positive autoregulatory loop maintaining gene expression levels. Here, we show that the mutant *compacta* (*co*), whose vegetative growth and petal size are affected, plays a role in B function. Late events in petal morphogenesis such as development of conical cell area and scent emissions were reduced in *co* and *def*^{nicotianoides} (*def*^{nic}), and absent in *co def*^{nic} double mutants, suggesting a role for *CO* in petal identity. Expression of *DEF* was down-regulated in *co* but surprisingly *GLO* was not affected. We investigated the levels of *DEF* and *GLO* at late stages of petal development in the *co*, *def*^{nic} and *glo-1* mutants, and established a reliable transformation protocol that yielded *RNAi-DEF* lines. We show that the threshold levels of *DEF* or *GLO* required to obtain petal tissue are approximately 11% of wild-type. The relationship between *DEF* and *GLO* transcripts is not equal or constant and changes during development. Furthermore, down-regulation of *DEF* or *GLO* does not cause parallel down-regulation of the partner. Our results demonstrate that, at late stages of petal development, the B function transcriptional network topology is not based on positive autoregulation, and has additional components of transcriptional maintenance. Our results suggest changes in network topology that may allow changes in protein complexes that would explain the fact that not all petal traits appear early in development.

Keywords: *Antirrhinum majus*, B function, autoregulatory loop, network topology, floral size, floral scent.

INTRODUCTION

Seminal work in *Antirrhinum majus* and *Arabidopsis thaliana* allowed formulation of a combinatorial model based on gene functions explaining what later was found to be a general scheme of floral organ development in angiosperms (Schwarz-Sommer *et al.*, 1990; Coen and Meyerowitz, 1991; Egea Gutierrez-Cortines and Davies, 2000; Causier *et al.*, 2010). The so-called ABC model has been tested and interpreted in various forms in several plant species. B function genes are involved in petal and stamen morphogenesis, and two genes, *DEFICIENS* and *GLOBOSA*, perform this task in *Antirrhinum* (Sommer *et al.*, 1990; Trobner *et al.*, 1992).

Petal development involves several subsets of genes activated by the B function. Amongst the features of a fully mature petal are the distinct colours displayed, resulting from pigment synthesis and down-regulation of chlorophyll production, proper size and shape, and release of scent. Petal development is not a linear process. The phenylpropanoid synthesis pathway involved in petal pigmentation does not show simple activation, but instead follows a pattern of early and late gene expression (Martin and Gerats, 1993). This is true in *Antirrhinum* and *Petunia*, indicating that some fine regulatory aspects of petal development may be conserved in evolution (Almeida *et al.*, 1989; Martin *et al.*, 1991; Weiss *et al.*, 1993). Petal growth also displays bi-phasic behaviour in *Petunia*, *Gerbera* and Arabidopsis, with petal development promoted by cell division and later stages promoted by cell expansion (Reale *et al.*, 2002; Anastasiou and Lenhard, 2007; Laitinen *et al.*, 2007). In

Antirrhinum, petal growth is somewhat more complex, as cell division occurs in early stages and regions where cell division occur are also detected late in development (Perez-Rodriguez *et al.*, 2005; Delgado-Benarroch *et al.*, 2009a).

At later stages, petal epidermal cells become conical as a result of expression of the *MIXTA* gene (Noda *et al.*, 1994). This process is conserved among species, and both conical cell development and the angle of petal reflection are controlled partly by *MIXTA* in *Antirrhinum* and *Petunia* (Baumann *et al.*, 2007). Conical cell formation in *Antirrhinum* continues until late stages of petal development, well after anthesis and before petal abscission (Goodwin *et al.*, 2003). *MIXTA* and *MIXTA-LIKE* genes have a conserved function in conical cell development during evolution (Di Stilio *et al.*, 2009). *MIXTA* expression is known to be controlled by B function genes, as plants expressing unstable alleles of *def* have been shown to display conical cells in reverting sectors (Carpenter and Coen, 1990). The level of expression of *MIXTA* and *MIXTA-LIKE-1* depend on the quantitative levels of *DEF* and *GLO* in *Antirrhinum* (Perez-Rodriguez *et al.*, 2005). Conical cells have several biological functions related to pollinator attraction, including scent production (Kolosova *et al.*, 2001; Whitney *et al.*, 2009a,b, 2011). The complex floral scent profile of most plants is the result of unique blends of compounds, whose production is due to activation of several biochemical pathways (Vainstein *et al.*, 2001). The *Antirrhinum* scent profile includes methyl benzoate, a product of the phenylpropanoid synthesis pathway, and terpenoids such as myrcene and ocimene (Dudareva *et al.*, 2000, 2003).

Activation of floral homeotic genes in Arabidopsis requires two partially redundant paralogs, *APETALA1* (*AP1*) and *CAULIFLOWER* (Kempin *et al.*, 1995; Ferrandiz *et al.*, 2000). Negative regulation of the genes *AGAMOUS-LIKE24* (*AGL24*) and *SHORT VEGETATIVE PHASE* (*SVP*) by *AP1* is required to activate *SEPALLATA* (*SEP*) (Kaufmann *et al.*, 2010b). The *SEP1–4* family is important to activate B function in *Petunia*, tomato and Arabidopsis (Angenent *et al.*, 1993; Pnueli *et al.*, 1994; Pelaz *et al.*, 2000; Vandenbussche *et al.*, 2003). The resulting B function activity is maintained by a positive autoregulatory loop that has been described in *Antirrhinum*, *Petunia* and Arabidopsis (Schwarz-Sommer *et al.*, 1992; Halfter *et al.*, 1994; Zachgo *et al.*, 1995; Honma and Goto, 2000; Vandenbussche *et al.*, 2004). The B function gene products form heterodimers (Davies *et al.*, 1996b; Winter *et al.*, 2002; Wang *et al.*, 2010) that can bind their own promoters and activate transcription. Plants expressing hypomorphic alleles of *def* display progressively smaller petals that become more sepalloid with the strength of the alleles (Schwarz-Sommer *et al.*, 1992; Zachgo *et al.*, 1995; Bey *et al.*, 2004). Petal growth as a whole is affected in B function homeotic mutants. Plants expressing null $def^{globifera}$ (def^{gli}) and *glo-1* alleles display second-whorl organs that are indistinguishable from first-whorl sepals (Trobner *et al.*, 1992), and sepals are much shorter than petals in *Antirrhinum majus* (Delgado-Benarroch *et al.*, 2009a). As a result of the studies described above and others performed in Arabidopsis (Szecsi *et al.*, 2006; Kaufmann *et al.*, 2009), there is a general agreement that floral organ size requires proper function of the floral organ identity genes (Yu *et al.*, 2004; Dornelas *et al.*, 2011).

Although positive autoregulatory loops occur as network motifs in many biological pathways (Heintzen *et al.*, 1997; Varghese and Cohen, 2007; Fujiwara *et al.*, 2009), they are inherently slow to respond to variation of gene expression (Kalir *et al.*, 2005; Alon, 2007), which may result in decreased flexibility (Ma *et al.*, 2006). Given the importance of the B function in terms of petal and stamen identity, it is possible that B function transcriptional maintenance includes gene activation, positive autoregulatory loop control and some parallel or ancillary components that add robustness to the system. Indeed, the obligate heterodimerization of canonical B function gene products adds robustness to the system at the post-transcriptional level (Espinosa-Soto *et al.*, 2004; Lenser *et al.*, 2009; Kaufmann *et al.*, 2010a; Geuten *et al.*, 2011). Further robustness is probably achieved as a result of larger MADS box complexes, which may aid in stabilization of the protein–DNA binding complexes (Egea-Cortines *et al.*, 1999; Theissen and Saedler, 2001; Melzer and Theissen, 2009; Kaufmann *et al.*, 2010a). Despite these protein stabilization processes, decreases in B function gene expression cause clear homeotic changes in *Antirrhinum*, *Petunia* (Vandenbussche *et al.*, 2004; Rijpkema *et al.*, 2006) and Arabidopsis (Irish and Yamamoto, 1995), demonstrating the importance of sustained transcriptional activity of the B function.

Although the initial steps of petal development are understood in some detail, late stages of development are thought to be a follow-up, but, to the best of our knowledge, no quantitative analysis of B function transcription at late stages of petal development has been performed to support this hypothesis.

Here we report genetic characterization of the mutant *compacta*, a classic *Antirrhinum majus* mutant (Kuckuck and Schick, 1930) in which leaf shape and floral size are affected. We uncover a genetic interaction of *co* with *def* that implicates *CO* in activation of *DEF* expression. We measured scent production in the *co* and def^{nic} mutants, and found that production of methyl benzoate, ocimene and myrcene was reduced in *co* and def^{nic} mutants and was completely absent in *co* def^{nic} double mutants, demonstrating a role for *co* in B function. In order to establish the threshold of B function, we developed a highly reliable transformation protocol and obtained *RNAi-DEF* lines. We performed quantitative expression analysis of *DEF*, *GLO* and *MIXTA* in *co* def^{nic} double mutants, *glo-1* and *RNAi-DEF* lines. We identified the thresholds of *DEF* and *GLO* associated with different levels of petal identity, and surprisingly found that

the levels of *DEF* and *GLO* transcripts changed at later stages of development, which was unexpected from a network topology based exclusively on positive autoregulation. We propose a model of B function transcriptional control that accommodates the data presented and may explain petal development as a multistep process.

RESULTS

The *co* mutation affects petal and stamen cell size

The mutant *compacta* had been described as a recessive mutant (Stubbe, 1966), and segregation analysis of a cross of *co* with the laboratory wild-type line 165E confirmed this result (Schwarz-Sommer *et al.*, 2010). As previously described, we found that the *co* mutation affected vegetative growth, including decreased internode elongation and smaller leaves that were altered both in width and length (Table 1). Leaf number until the first flower was not different from wild-type, indicating that the *co* mutation does not affect floral transition.

The flowers of *co* plants may be easily distinguished from those of wild-type because stamens protrude outside the tube (Figure 1a). Furthermore, they were significantly smaller than those of wild-type (Figure 1b,c and Table 2) for all floral parameters analyzed, except for the adaxial stamens, which retained wild-type size (Figure 1d). In many cases, under greenhouse conditions, the adaxial protruding stamens tended to show dehiscence and dehydration before the flowers were fully open. Furthermore, the abaxial stamens appeared more separate than in wild-type, forming a characteristic V shape (Figure 1d). Hand self-pollinated *co* flowers were fully fertile. Flower colour was not affected in *co* mutants, which displayed colour segregation of the *nivea*, *delila* and *pallida recurrens* loci (Figure S1) present in the 165E and Sippe50 wild-type background.

We investigated the effects of the *co* mutation on cell division and expansion in the various floral organs. Sexual organs in the *co* mutant showed independent cellular phenotypes, as cells in stamens were significantly smaller than in wild-type, whereas cell size in styles was not affected (Figure 2 and Table 3). With regard to petals, flat cells proximal to the tube did not show significant differences with respect to wild-type flowers. However, in the distal part of the petal, conical cells were 43% smaller than in wild-type, and flat cells showed a decrease in area of 33%. Altogether, the observed petal phenotypes may be explained by a decrease in cellular size in the petals (Figure 2 and Table 3).

Co plays a role in B function

As petal and stamen cell size were significantly reduced in the *co* mutant, we investigated a possible interaction with organ identity. We crossed *co* with the weak allele *def*^{nic}. This allele affects second- and third-whorl organ identity, with sepaloid petals that are smaller than wild-type petals but still develop colour and conical cells (Schwarz-Sommer *et al.*, 1992). We constructed an F_2 population of *co* × *def*^{nic}, obtaining a Mendelian segregation of 47 wild-type, 17 *co*, 19 *def*^{nic} and seven plants with a stronger phenotype (χ^2 = 0.8642, d.f. = 3, P = 0.8341). The plants with floral phenotypes differing from *co* or *def*^{nic} single mutants were considered *co def*^{nic} double mutants. The phenotype resembled *def*^{nic} but was more extreme, in some cases showing second-whorl sepalloid organs resembling those of *def*^{gli} null mutants (Figure 3a–c). We selfed *co* mutant siblings of the putative double mutants and obtained a segregation of 3:1 for plants displaying an enhanced *def*^{nic} phenotype, thus confirming that the effect of the *co* mutation is an enhancement of *def*^{nic}. The *CO* gene is not allelic to *DEF* based on the F_1 phenotypes that were wild-type and the fact that these genes map to linkage groups 6 and 8, respectively (Schwarz-Sommer *et al.*, 2010).

We compared organ size in *co* mutants and *co def*^{nic} double mutants, and found that all measured parameters were significantly smaller except first-whorl sepals (Table 2), indicating a synergistic effect of the *co* and *def*^{nic} mutations. The most prominent decreases in size in the second whorl corresponded to the tube length and lateral expansion of the abaxial petals, which showed mean reductions >60% (P < 0.001). Furthermore, *co def*^{nic} double mutants completely lacked the typical *Antirrhinum* petal palate. Modest but significant reductions in size were found in the third whorl, which showed partial carpelloid structures, although stamens were formed in all flowers analyzed.

We examined cellular morphologies and sizes in petals of *def*^{nic}. As previously described, *def*^{nic} mutants showed a range of cells reminiscent of wild-type sepal and petal cell types. We observed typical puzzle cells seen in sepals, with a

Table 1 Comparison of vegetative parameters between wild-type and the *co* mutant

	Internode (mm)			Leaf 1 (mm)		Leaf 2 (mm)		Leaf 3 (mm)		Number of leaves		
Genotype	1	2	3	Length	Width	Length	Width	Length	Width	Decussate	Spiral	Total
co	10.43.4	16.8 ± 7.4	21 ± 4.9	16.1 ± 2.2	11.2 ± 1.2	25.9 ± 1.5	15.6 ± 1.0	35.5 ± 5.9	16 ± 2.4	8.8 ± 1.2	5.2 ± 4.1	14 ± 4.0
Wild-type	18.9 ± 1.9	27.2 ± 3.2	31.8 ± 4.3	24.1 ± 2.1	13.4 ± 0.8	39 ± 2.9	19.4 ± 1.6	46.1 ± 4.9	18.9 ± 2.9	8.1 ± 1.3	3.7 ± 2.7	11.8 ± 1.8
%	−45.16***	−38.41***	−33.89***	−33.22***	−16.39***	−33.57***	−19.36***	−23.01***	−15.48*	8.64	40.54	15.71

Values of internode size and leaves are means ± standard deviation (n = 15). Percentages refer to wild-type siblings in the F_2 segregating population. Asterisks indicate significant differences between the *co* mutant and wild-type: *P < 0.05; **P < 0.01; ***P < 0.001.

Figure 1. Wild-type (left) and *co* mutant flowers (right) from the side, and longitudinal sections.

gradient towards the distal portion of the petal that started with flat oval-shaped cells that increased gradually in size until true conical cells formed at the edges of the petaloid organs (Figure 4). Both the size of the conical cells and the overall surface of the petal were greatly reduced compared to wild-type petals or *co*. In contrast, we did not find conical cells in *co def*^{nic} double mutant flowers, which displayed both puzzle cells and flat cells. Differences in cell morphology between the *co* mutant and the *co def*^{nic} double mutant were pronounced enough not to permit legitimate comparison of cell sizes. The lack of conical cells in *co def*^{nic} double mutants strongly suggests that *co* itself plays a role, not only in determination of cell size, but also in late petal development. Cells in the third whorl of *co def*^{nic} double mutants showed a decrease in size beyond that found for *def*^{nic} single mutants. The fourth-whorl style cells in wild-type and *co* were not significantly different (Table 3). However, the *co def*^{nic} double mutant had larger cells than *def* single mutants despite the fact that this organ is smaller (Table 4). This suggests that *co* may interact with other genes involved in carpel and stamen development such as *PLENA* and *FARINELLI* (Bradley *et al.*, 1993; Davies *et al.*, 1999).

Co plays a role in scent production

We measured the production of three major scent compounds (myrcene, ocimene and methyl benzoate) in fully developed flowers of a segregating population of *co* and *def*^{nic}, 24 h after anthesis (Table 5 and Figure S2). We observed emission of the three compounds in wild-type flowers. However, we did not find myrcene in any of the *co* samples analyzed, and the levels of emission of ocimene and methyl benzoate were similar to those of wild-type. In *def*^{nic} flowers, we found levels similar to wild-type for myrcene, whereas ocimene and methyl benzoate were drastically reduced. The phenotype of the *co def*^{nic} double mutant was extreme concerning scent emission, as we were not able to detect myrcene, ocimene or methyl benzoate in any of the samples analyzed.

Co is involved in *DEF* transcriptional control and plays a role in B function

As the *co* mutant showed a number of phenotypes that may be described as B function-related, we investigated the effect of the *co* mutation on the B function transcriptional network by quantitative gene expression analysis. We found that *DEF* gene expression was significantly down-regulated in *co* mutants to 11.6% of the value found in wild-type ($P = 0.04$; Figure 5a), similar to the down-regulation in *def*^{nic} ($P = 0.653$) versus wild-type. Surprisingly, the levels of *GLO* expression were higher in *co* than in wild-type, but not significantly ($P = 0.23$). This finding is contrary to what would be expected from a positive autoregulatory loop scheme (Schwarz-Sommer *et al.*, 1992), which suggests simultaneous down-regulation of *GLO* as observed in *def*^{nic} ($P = 0.029$). These unexpected results indicate that *CO* is involved in the activation or maintenance of *DEF* expression, whereas *GLO* is not directly affected. In the *co def*^{nic} double mutant, both *DEF* and *GLO* expression were down-regulated compared to wild-type. Furthermore, the high levels of *GLO* in the *co* mutant may be partly responsible for the better petal development observed compared to *def*^{nic}, but the results for the double mutant indicate that *CO* also plays a downstream role, beyond the uncovered effect on *DEF* expression, and may

Table 2 Comparison of floral parameters for wild-type, the *co* mutant, the *def*^{nic} single mutant and the *co def*^{nic} double mutant

Genotype	Tube length (mm)	Lower length (mm)	Petal height (mm)	Sepal length (mm)	Tube width (mm)	Upper (total) length (mm)	Lower petal expansion (mm)	Upper petal expansion (mm)	Stamen length (mm)	Gynoecium length (mm)
Wild-type	17.9 ± 0.7	30.8 ± 2.7	26.4 ± 2.7	7.9 ± 0.8	12.1 ± 0.8	39.5 ± 0.9	26.2 ± 1.6	29.9 ± 2.0	25.6 ± 0.9	22 ± 0.7
co	15.3 ± 0.8	23.5 ± 1.3	17.1 ± 2.3	6.6 ± 0.5	10.4 ± 0.7	28.3 ± 1.4	19.2 ± 2.7	16.4 ± 2.3	26 ± 1.8	20.1 ± 1.0
def ^{nic}	8.7 ± 4.9	20.5 ± 2.0	11.2 ± 1.9	6.4 ± 0.6	7.1 ± 0.5	20.8 ± 2.3	15.8 ± 2.9	11.7 ± 2.3	16.6 ± 1.3	19.3 ± 2.3
co def ^{nic}	5.3 ± 0.5	11.4 ± 1.7	8.1 ± 1.0	7.2 ± 0.8	5.7 ± 0.5	12.0 ± 1.9	7.6 ± 1.5	8.1 ± 0.8	14.8 ± 0.6	16.9 ± 0.9
% *def*^{nic} versus *co def* ^{nic}	−38.38*	−44.64***	−27.93***	12.80	−19.26***	−42.25***	−51.82***	−30.37**	−10.62**	−12.17*
% *co* versus wild-type	−15.07***	−23.64***	−35.01***	−16.48***	−14.03***	−28.37***	−26.93***	−45.09***	1.40	−8.68***

Total number of measurements for each parameter = 10. Values are means ± standard deviation. Asterisks indicate significant differences using the wild-type or *def* ^{nic} single mutant as: *P < 0.05; **P < 0.01; ***P < 0.001.

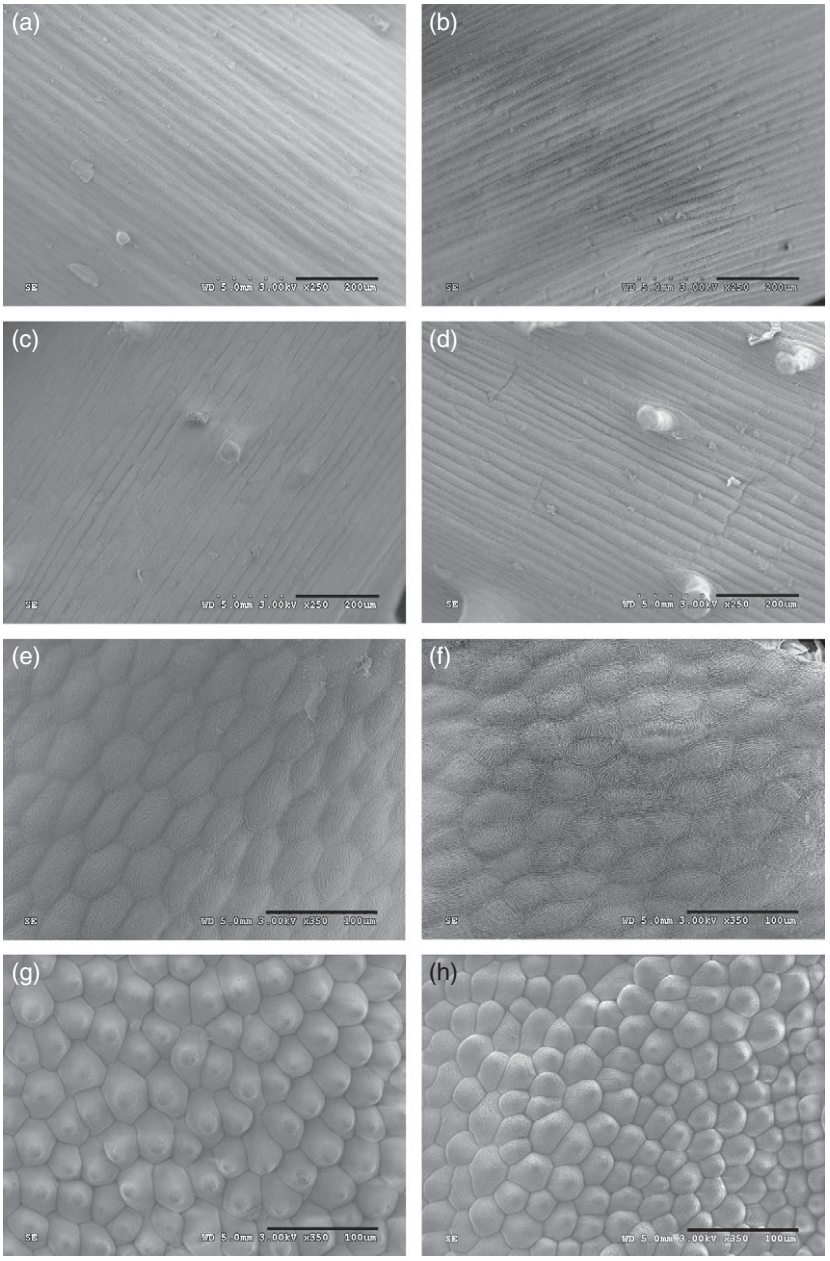

Figure 2. Scanning electron microscopy of cells from various organs of fully developed flowers of wild-type (left) and *co* mutant flowers (right). (a, b) Third-whorl styles, (c, d) fourth-whorl gynoecium, (e, f) dorsal petal, proximal to the tube, and (g, h) dorsal petal, distal part. Scale bars = 100 μm.

Table 3 Cell area of petal, stamen and style in wild-type and the *co* mutant

			Petal (μm^2)	
Genotype	Stamen (μm^2)	Style (μm^2)	Conical cells	Flat cells
co	2948.4 ± 103.9	2123.1 ± 85.1	756.9 ± 29.0	1609.66 ± 52.19
Wild-type	3568.1 ± 76.4	2221.9 ± 70.5	1346.5 ± 43.3	2101.24 ± 55.83
%	−17.37*	−4.45	−43.78*	−23.39*

Total number of cells measured for each organ/mutant = 50. Values are means ± standard error. Asterisks indicate significant differences between the *co* mutant and wild-type: *$P < 0.05$.

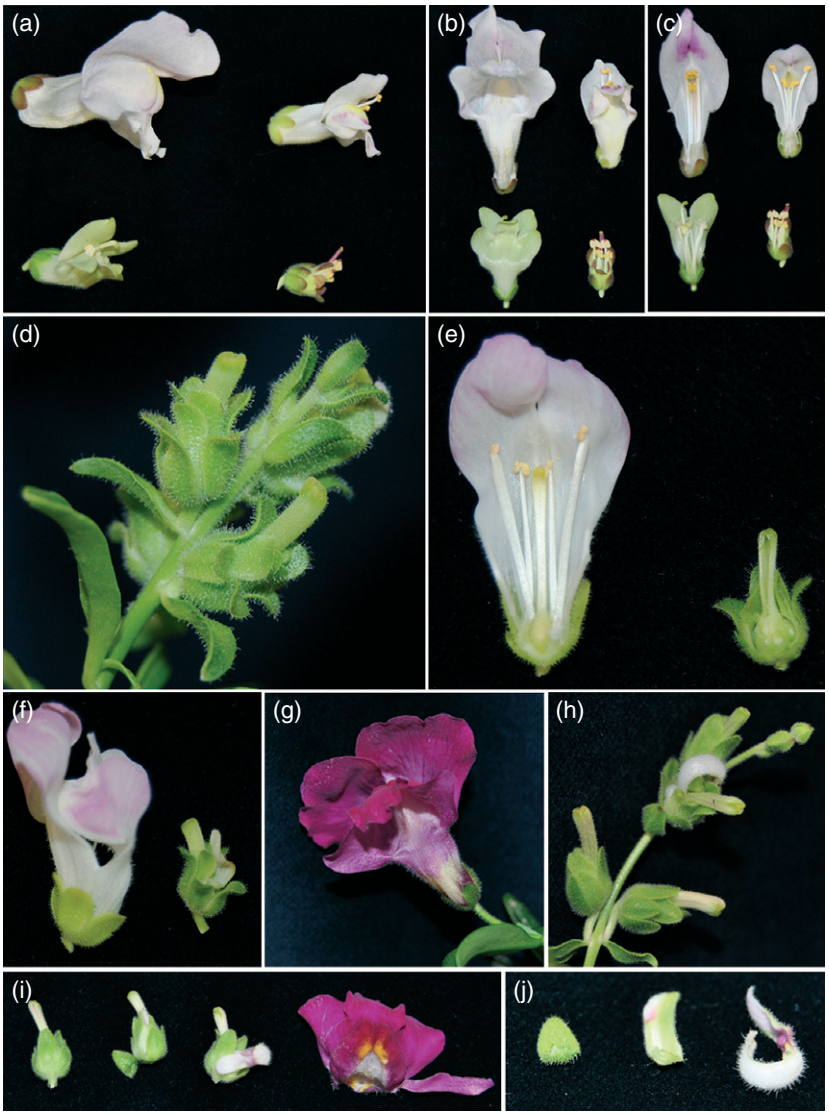

Figure 3. Phenotypes and lines.
(a–c) Top left, wild-type; top right, the *co* mutant; bottom left, *def*^{nic}; bottom right, *co def*^{nic} double mutant.
(d) *RNAi-DEF* transgenic line showing extreme phenotypes similar to the classic *def*^{gli} null allele.
(e) Section of wild-type (left) and the *RNAi-DEF* strong phenotype line (right).
(f) Wild-type (left) and partially reverting *RNAi-DEF* flower with chimeric second-whorl organ (right).
(g) *RNAi-DEF* flower with wild-type appearance.
(h) *glo-1* mutant showing a revertant second-whorl organ.
(i) Comparison of *glo-1* flowers, showing two without reversion, one with a partial petaloid structure in the second whorl, and a petal with wild-type appearance from the *RNAi-DEF* line.
(j) Close-up of increasingly wild-type second-whorl organs from *glo-1* flowers.

be considered a B function gene itself, supporting the previous data on cell types and scent emission.

Quantitative analysis of transcriptional regulatory network in late petal development

In order to obtain a comprehensive picture of gene expression levels of *DEF* and *GLO*, and identify the quantitative thresholds supporting different degrees of petal development, we used a mixture of genetic backgrounds. We developed an improved protocol to transform *Antirrhinum majus* (see Experimental procedures and Appendix S1), and obtained two independent transgenic lines harbouring an *RNAi-DEF* construct that were positive for kanamycin resistance and showed a range of phenotypes from weak to null

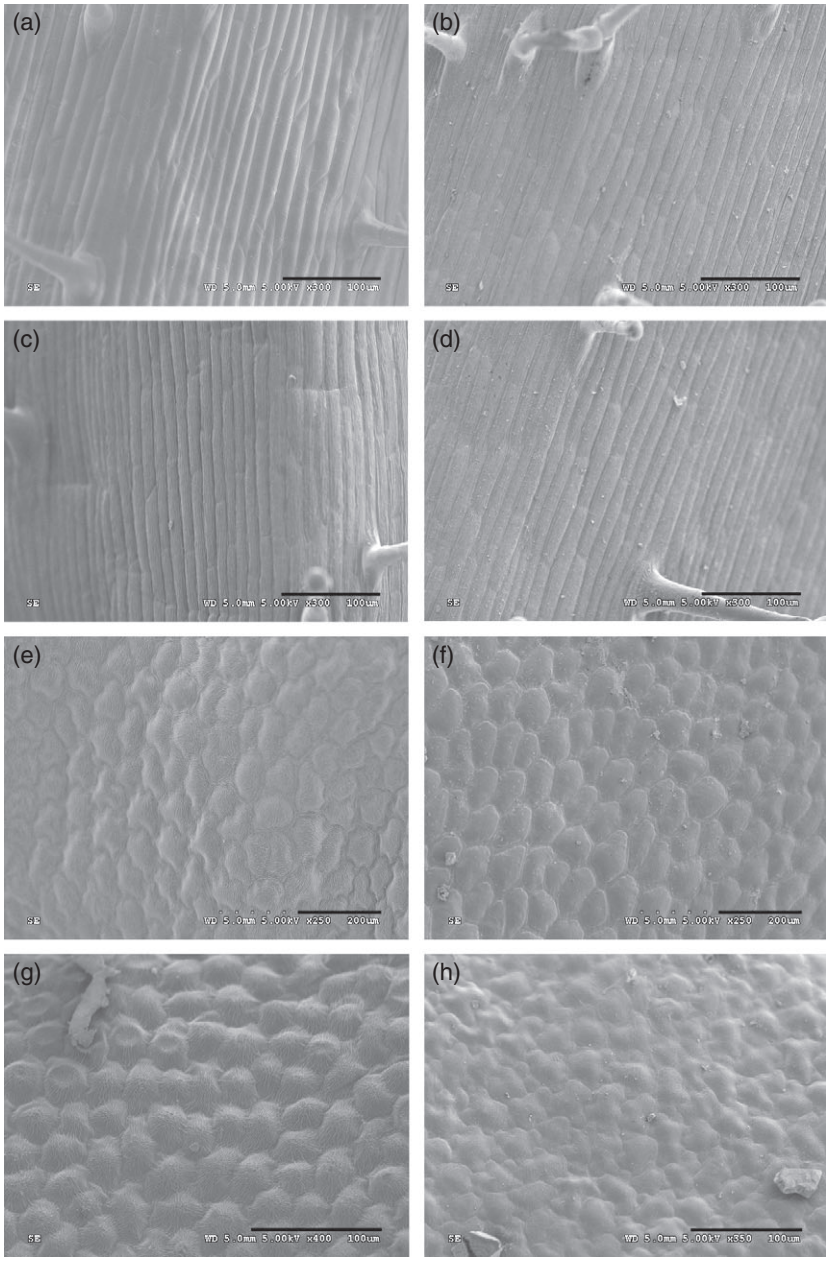

Figure 4. Scanning electron microscopy of floral organs of *def* ^{nic} mutant (left) and *co def* ^{nic} double mutant (right).
(a, b) Third-whorl organs, (c, d) gynoecia, (e, f) dorsal petal proximal region of flat cells, and (g, h) dorsal petal distal region of conical cells. Scale bars = 100 μm.

def alleles (Figures 3d and S3). Flowers of the strongest line showed two whorls of sepals and a third whorl of carpels, typical of a *def*^{gli} allele (Figure 3e). In a direct comparison, they could not be distinguished from flowers expressing *def*^{gli} or *glo-1* null alleles. The strongest line showed progressive acropetal loss of the extreme phenotype, displaying flowers with second-whorl sepal/petal chimeric organs (Figure 3f), and eventually reverted completely to produce apparent wild-type flowers (Figure 3g).

We gathered second-whorl organs from the aforementioned single and double mutants and the strong *RNAi-DEF* line. In order to obtain additional samples from revertant tissue, we established a greenhouse plot of plants expressing the *glo-1* unstable allele for several years, and obtained revertant flowers with second-whorl chimeric organs (Figure 3h–j) during the spring under southern Spain growing conditions.

We analyzed the levels of *DEF* and *GLO* expression in the second-whorl organs of the transgenic line displaying the strongest phenotype by quantitative RT-PCR, and found that expression was reduced to 2% of wild-type, as expected for organs that were completely transformed into sepals (Figure 5). The smallest second-whorl chimeric organs recovered (sepal/petal) displayed levels of *DEF* expression at a level that was 14% of that of the wild-type (P = 0.029) (Figure 5a). Furthermore, the two independent RNAi lines

Table 4 Cell area of stamen and style in the *def*^{nic} single mutant and the *co def*^{nic} double mutant

	Stamen filament (μm^2)	Style (μm^2)
Wild-type	3568.09 ± 154.43	2221.99 ± 70.49
def^{nic}	2213.4 ± 96.5	1466.9 ± 76.2
co def^{nic}	1940.5 ± 76.6	1842.2 ± 70.3
% *co* versus *wild-type*	−17.37***	−4.45
% *def*^{nic} versus *co def*^{nic}	−12.33*	+25.58***

Total number of cells measured for each organ/mutant = 50. Values are means ± standard error.
Asterisks indicate significant differences using the wild-type or *def*^{nic} single mutant as: *$P < 0.05$; ***$P < 0.001$.

Table 5 Effect of the *co* and *def*^{nic} mutations on volatile levels

Genotype	Myrcene	Ocimene	Methyl benzoate
Wild-type	40.2	251.2	137.2
co	ND	156.6	165.4
def^{nic}	34.4	9.7	29.6
co def^{nic}	ND	ND	ND

Quantities refer to mean emissions of three samples (ng g^{-1} tissue h^{-1}). ND indicates that we could not detect the compound in any sample.

displayed an interesting feature in that the first flowers showed a *def* phenotype that was lost later on, indicating that an acropetal gradient could overcome the RNAi-dependent decrease in gene expression. Independent transgenic experiments with other genes indicate that this was a feature of the *RNAi-DEF* construct but is not a general feature of *Antirrhinum* stably transformed lines (M.M.-R., unpublished observations). *RNAi-DEF* flowers with a wild-type appearance had *DEF* and *GLO* expression levels similar to wild-type. The *glo-1* allele shows instability, and we compared it against the *RNAi-DEF* plants and the series of *co* and *def*^{nic} mutants. The results obtained show that the levels of *DEF* in *glo-1* were between 11 and 31% of wild-type in sepal and sepal/petal organs, with 22% in revertant petals and wild-type levels of expression in near-wild-type looking petals. In contrast, *GLO* levels did not fully recover the wild-type expression levels, showing levels that were always significantly lower than in wild-type petals.

Our data shows that thresholds of 11–15% of wild-type levels of expression of *DEF* or *GLO* are associated with development of recognizable petal tissue.

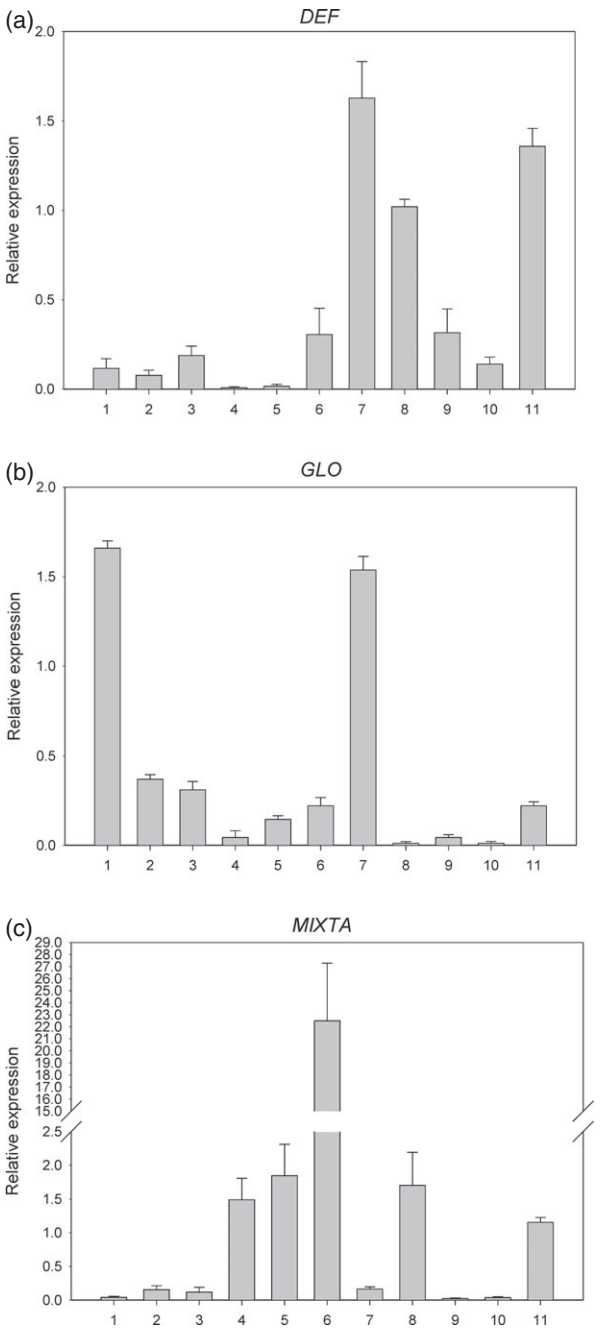

Figure 5. Relative expression of (a) *DEFICIENS*, (b) *GLOBOSA* and (c) *MIXTA* in second-whorl organs compared to wild-type petals.
An arbitrary level of 1 was assigned to the wild-type: 1, the *co* mutant; 2, *def*^{nic}; 3, *co def*^{nic} double mutant; 4, *RNAi-DEF* sepal; 5, *RNAi-DEF* petal/sepal; 6, *RNAi-DEF* petal; 7, *RNAi-DEF* petal (normal flower); 8, *RNAi-DEF* tube; 9, *glo-1* sepal; 10, *glo-1* revertant; 11, *glo-1* petal.

Reciprocal *DEF* and *GLO* transcript levels change during development

Although the currently supported hypothesis of B function is based on a positive autoregulatory loop of two B function gene products, a direct comparison of mRNA levels for *DEF* versus *GLO* has not been reported, and examination of the levels of *DEF* and *GLO* in the tissues analyzed indicated that important differences may exist in the reciprocal levels of expression. Thus we used the data obtained to perform a nested calculation allowing direct comparison of *DEF* versus *GLO* in each sample. We used a large sample for quantitative RT-PCR: 20 biological samples with three technical

replicates comprising ten wild-type flowers at developmental stage 13–14, i.e. approximately 1 cm long and still closed (Vincent and Coen, 2004), and ten wild-type fully open flowers 1 day after anthesis. The reason for this was that sampling of revertant and transgenic tissue necessarily has to be performed when development is complete and the phenotypes are distinguishable, but we wished to identify possible ontogenic changes in reciprocal levels of *DEF* and *GLO* gene expression. A simple inspection of the data from closed flowers showed that, contrary to what was expected, transcriptional levels of *DEF* and *GLO* were not equal. *GLO* gene expression in petals was significantly lower than that of *DEF* in four of ten samples. Combining all samples indicated a level for *GLO* transcripts of 0.806 relative to *DEF* ($P = 0.013$), with most values below 1.0 (Figure 6 and Table 6). Surprisingly this unequal relationship for *GLO* versus *DEF* expression levels resulted in significantly higher expression of *GLO* in petals when flowers were open (1.847; $P = 0.000$). We compared two samples of gene expression data that had equal variances (Fligner–Killeen test, $P = 0.5541$), and found that, as expected from the data inspection, the relationships between *DEF* and *GLO* expression in closed and open flowers are significantly different (*t*-test, $P = 5.765e\text{-}06$). The data show that, from middle to late stages of development, the relationship between *DEF* and *GLO* transcription varies significantly, with a marked up-regulation of *GLO* compared to *DEF*.

In *glo-1* revertant petals, *DEF* and *GLO* expression levels were close to 1. However, *DEF* and *GLO* levels were dissimilar in the rest of the samples analyzed (Table 6). In perfectly formed petals of *RNAi-DEF* plants, *GLO* expression was at least 11-fold higher than *DEF*. These large differences between *DEF* and *GLO* expression were also found in *co* petals, indicating that disparity in gene expression between *DEF* and *GLO* may be tolerated and still give rise to petal tissue. In the rest of the samples with strong homeotic alterations, differences between *DEF* and *GLO* ranged between fivefold in *co def*^{nic} double mutants to close to 100-fold in the strongest homeotically transformed organs, i.e. sepal/petal organs of *RNAi-DEF* or second-whorl sepals of *glo-1*. Our results show that, in wild-type flowers, *DEF* and *GLO* expression is not matched, and the large differences between the two genes in terms of gene expression in the array of tissues analyzed cannot be completely reconciled if we assume a positive autoregulatory loop as the sole form of B function transcriptional maintenance.

Effect of the *co* mutation and B function manipulation on downstream processes

As *MIXTA* is a well-defined downstream target of B function, and the *co* mutation affected the area of conical cells, we measured *MIXTA* gene expression and found that levels of *MIXTA* in the *co* mutant were as low as 4.1% of the wild-type (Figure 5). These low levels were also found in second-whorl sepals of *glo-1*, *glo-1* revertant sepal/petal tissues and *RNAi-DEF* normal flowers. However, the other *RNAi-DEF* tissues showed higher levels of *MIXTA* expression, indicating that, although the levels of *DEF* and *GLO* were significantly lower than in wild-type, there may be other factors involved requiring further analysis.

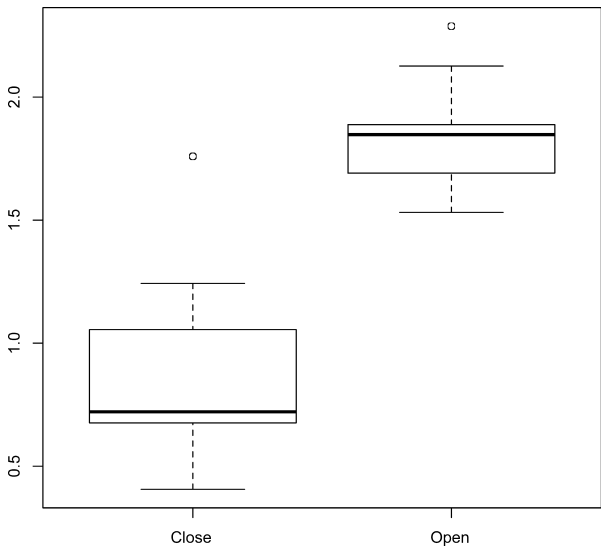

Figure 6. Box plot of expression values for *GLO* versus *DEF* in closed and open flowers.
The *y* axis refers to *GLO* expression values compared to *DEF* having an arbitrary value of 1.

Table 6 Expression of *GLO* compared to *DEF* in various tissues

Organ	Relative *GLO* expression	*P* value
Wild-type closed, stage 13	0.806	0.013
Wild-type, open	1.847	0.000
co	13.375	0.001
def^{nic}	20.128	0.0020
co def^{nic}	6.824	0.0010
RNAi-DEF petal (small)	6.465	0.003
RNAi-DEF petal/sepal	98.632	0.001
RNAi-DEF sepal	60.537	0.0000
RNAi-DEF tube	8.05	0.234
RNAi-DEF (normal flower)	12.36	0.0010
glo-1 sepal	0.093	0.001
glo-1 revertant	0.617	0.491
glo-1 petal	1.057	0.695

An arbitrary value of 1 was assigned to each tissue for the level of *DEF*.

DISCUSSION

A quantitative component of homeotic gene function

As the ABC model is based on spatial restriction of gene expression, much information has been generated to explain the discrete gene expression patterns. Many mutants identified show homeotic changes caused by lack

of expression of the ABC genes. Less well characterized are the quantitative requirements for floral organ identity genes. The original hypothesis developed in *Antirrhinum* postulates that *DEF* and *GLO* transcription occurs in an initial step, and self-maintained gene expression levels take over the initial activation to run the developmental program until organ development is complete.

Our data shows that levels of *DEF* or *GLO* mRNA of 11% or above can support development of recognizable petal tissue. However, these levels do not sustain full organ size. The fact that the palate is completely absent in many *def*^{nic} flowers and all *co def*^{nic} double mutants indicates that different regions of the petal also require different thresholds of B function for development or have different levels of expression of B function along the petal area. The effects on late developmental stages are even more pronounced, as the finding of *MIXTA* expression levels of 4% of the wild-type in the *co* mutant or 16% in *RNAi-DEF* revertant petal confirms previous work that established the quantitative importance of *DEF* expression for *MIXTA* expression (Perez-Rodriguez *et al.*, 2005). Reduced expression of the C function gene *AGAMOUS* (*AG*) in Arabidopsis by RNAi plants and plants expressing several *ag* alleles analyzed have shown that threshold levels of *AG* have different effects on organ identity and meristem determinacy (Sieburth *et al.*, 1995; Causier *et al.*, 2009; Das *et al.*, 2009; Maier *et al.*, 2009), indicating that not all downstream processes require the same levels of expression. Furthermore, quantitative changes in gene expression modify the spatial expression of *AG* in Arabidopsis (Cartolano *et al.*, 2009), supporting the importance of quantitative gene expression levels for floral patterning and organ development.

The phenotypic effects of the *co* mutation on petal cell development clearly show a strong decrease in the area with conical cells, correlated with down-regulation of *MIXTA*. This decrease in the area comprising conical cells and the smaller size of the cells may explain the decrease in *MIXTA* expression. It may also explain a quantitative decrease in scent production, as benzoic acid carboxyl methyltransferase, which is involved in methyl benzoate production, is expressed in conical cells in *Antirrhinum* (Kolosova *et al.*, 2001). An additional role of *CO* downstream of *DEF* is supported by the finding that *def*^{nic} single mutants and *co def*^{nic} double mutants have similar levels of *DEF* and *GLO*, but the phenotypes analyzed are more extreme in the double mutant, suggesting that *CO* is a B function gene that is involved in activation or maintenance of *DEF*, and activation of part of the scent transcriptional network at late stages of petal development.

Determining the degree of homeotic transformation or petal organ identity has not been an easy task. Studies in Arabidopsis using ectopic expression of *PISTILLATA* (*Pi*) or its homolog from pea *PsPI* have used chimeric first-whorl organs comprising sepal and petal tissue as criteria to establish B function activity (Krizek and Meyerowitz, 1996; Berbel *et al.*, 2005). Indeed, model organisms such as *Petunia*, in which B function genes are duplicated, allow a much more detailed analysis. For instance, petal defects in plants expressing mutant alleles of *Phglo1* and *Phglo2* show greener and broader midvein, conversion of conical cells to sepal-like epidermal cells, or lack of stamen fusion to the petal tube (Vandenbussche *et al.*, 2004). Expression of the *TM6* gene from petunia under the control of a 35S promoter can rescue *Phdef* phenotypic defects to some extent, but still petals show a broad green midvein (Rijpkema *et al.*, 2006). Thus our approach of considering petal tissue as second-whorl organs that have recognizable regions resembling petals and are confirmed by scanning electron microscopy as having conical cells, fulfils a qualitative definition of the organ.

Determining what a petal is in terms of identity does not address the functional aspects. Petals have at least two recognizable functions: physical protection of the sexual organs during flower development, and insect attraction. Clearly these two functions do not necessarily overlap or have similar importance in all plants. Our data suggest that levels of *DEF* and *GLO* transcription above a threshold are required to obtain wild-type petal size, good development of conical cells, and scent production. Our data do not allow us to determine whether the reduction in scent is a result of decreased *MIXTA* expression that leads to fewer conical cells in which scent is produced, or whether it is a direct effect of *CO* or *DEF* and *GLO*. However, these possibilities are not mutually exclusive.

Structure of the B function regulatory network

A network topology based on a simple positive autoregulatory loop is not supported by the data obtained in the various tissues and genetic backgrounds described here. First, the *co* mutant has a strong effect on *DEF* but not on *GLO* gene expression, indicating that *CO* may be directly involved in *DEF* activation. *GLO* expression levels were maintained despite a decreased level of DEF–GLO heterodimer and increased basal promoter activity, indicating that other factors maintain *GLO* expression in the absence of positive autoregulation. This basal promoter activity may be flower-specific as *GLO* has well-defined expression patterns in petals and stamens (Trobner *et al.*, 1992; Zachgo *et al.*, 1995). In second-whorl organs with complete homeotic transformation, although the actual level of expression of *DEF* in *glo-1* or *GLO* in *RNAi-DEF* is significantly down-regulated compared to wild-type, the levels of expression of *GLO* compared to *DEF* in *RNAi-DEF* and *DEF* versus *GLO* in *glo-1* are significantly higher. This implies that the positive autoregulatory loop is only part of the B function maintenance, and a basal level of transcriptional activation is present for both *DEF* and *GLO*, at least at late stages of development. A graphical model describing the current model of transcriptional network and a new one based on the data presented in this contribution are shown in

Figure 7. Activation of B function consists of triggering *DEF* and *GLO* (Figure 7a), and such activation becomes independent at the middle and late stages of development (Figure 7b). Activation of *DEF* and *GLO* seem to be partly independent as *CO* only affects *DEF* (Figure 7c). Early experiments in tobacco showed a spatial difference in transcriptional activation of *NtDEF* and *NtGLO.* Ectopic expression of *DEF* and *GLO* causes ectopic expression of *NtDEF* in leaves and all floral organs, whereas *NtGLO* is ectopically expressed only in first-whorl organs (Davies *et al.*, 1996a). This indicates that positive autoregulation comprises organ-specific components and may differ between *DEF* and *GLO.*

We did not expect to observe differences in gene expression between *DEF* and *GLO*, and even more unexpected was the existence of developmental differences such as those found in the balance of the two transcripts. This also shows that the transcriptional network topology of B function changes during petal development, and is not a fixed entity as originally thought. However, petal growth and anthocyanin production are biphasic. Petal growth comprises cell division in early stages and cell expansion at later stages in different plants (Martin and Gerats, 1993; Reale *et al.*, 2002), whereas anthocyanin genes show early and late activation (Jackson *et al.*, 1992; Weiss *et al.*, 1993). Finally, scent production starts at anthesis. These obvious changes in the downstream targets of *DEF* and *GLO* cannot be explained by a simple model in which B function operates as a single-geared process. Our work has concentrated on transcriptional changes, but recent work has shown that translation rate constants play a dominant role in determining protein levels, and, combined with mRNA levels, account for 95% of the variance in protein quantities (Schwanhäusser *et al.*, 2011). This suggests that, if linear levels of translation rates are maintained during petal development for *DEF* and *GLO*, the changes in mRNA should translate into differing levels of protein.

Recent work has shown that quaternary complexes with diverse composition co-exist in Arabidopsis petals, indicating that there is an inherent flexibility in MADS-box tetramer formation (Smaczniak *et al.*, 2012). The developmental changes in the ratio of *DEF*/*GLO* expression levels may have implications with regard to the type of target genes that plant MADS box complexes recognize during petal development, and may explain the gradual developmental processes that occur during petal morphogenesis that lasts more than 20 days in *Antirrhinum*.

EXPERIMENTAL PROCEDURES

Plant material and genetics

The *compacta* and *deficiens nicotianoides* mutants were obtained from the Gatersleben collection (IPK Gatersleben, Gatersleben, Germany). The laboratory lines Sippe50, 165E and the *globosa* unstable allele *glo-1* (Trobner *et al.*, 1992) was obtained from Dr Zsuzsanna Schwarz-Sommer (Max-Planck-Institut für Pflanzenzüchtungsforschung, Köln, Germany). Plants were grown in the greenhouse as described previously (Bayo-Canha *et al.*, 2007). Homozygote mutants were crossed to obtain F_2 plants as described previously (Egea-Cortines *et al.*, 1999), and double mutants were identified by their phenotype (see Results) and the corresponding Mendelian segregation.

Microscopy

Fully developed flowers were harvested and analyzed as described previously (Delgado-Benarroch *et al.*, 2009b).

Constructs

We cloned a fragment of 207 bp encompassing the last 60 codons and 27 bp of the 3′ UTR of the *DEFICIENS* cDNA from *A. majus* into the pHellsgate12 plasmid (Helliwell and Waterhouse, 2003), using the primers DEF-forward (5′-GATGCAAGGAGAGAGGATC-3′) and DEF-reverse (5′-CTATAACATATATCGATCATACCATTAATT-3′) (Table S1). The hairpin construct of the pHellsgate12 vector was checked by PCR using an internal primer for the intron pH12-forward (5′-GTTGGCAGCATCACCCGA-3′) and pH12-reverse (5′-AAACTAGAAATTTACCTGCAC-3′) and a primer for the *DEF* gene in both directions.

Scent analysis

The volatile constituents in the flowers of the plants were separated and qualitatively identified by capillary gas chromatography/mass spectrometry (GC-MS).

For extraction of the volatile components, one cut flower per line was placed inside Falcon tubes for 24 h (DeltaLab, www.deltalab.es).

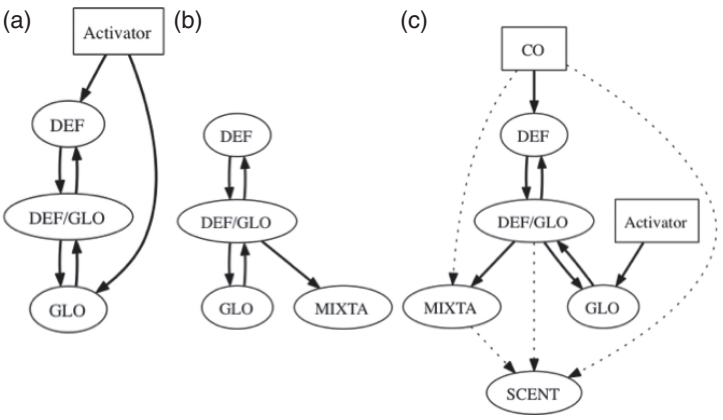

Figure 7. A graphical model of B function network topologies.
Initial steps of B function activation during early petal development (a), middle to late stages of petal development (b), and a newly proposed network topology for late stages of development (c). Rectangles refer to a transcriptional activation function. Dotted lines refer to direct activation that is possible but the current data do not allow discrimination between direct and indirect activation.

The tubes contained a suspended Twister™ bar (Gerstel GmbH & Co. KG, http://www.gerstel.de/), a magnetic stir bar of 10 mm length coated with 0.5 mm polydimethylsiloxane that had previously been conditioned.

Scent profiles were resolved on a 6890 gas chromatograph coupled to a 5975 inert XL mass selective detector (Agilent Technologies, http://www.home.agilent.com) equipped with a thermal desorption unit, a cooled injector system (CIS 4) and a multipurpose sampler (MPS2) (Gerstel GmbH & Co. KG).

The GC separation was performed on an HP-5MS UI capillary column (Agilent Technologies), 30 m, length × 0.25 mm, internal diameter x 0.25 μm (film) in constant pressure mode. The oven temperature was sequentially increased from 50 to 70°C at 5º per min, held for 1 min, and thereafter increased to 240°C at 10°C per min, with a holding time of 15 min. The inlet operated in solvent vent mode with a split ratio of 1:15. Chromatographic-grade helium was used as the carrier gas. We used *n*-pentadecane as an internal standard for qualitative analysis of the samples, adding 1 μl *n*-pentadecane (standard for gas chromatography, Fluka, Sigma-Aldrich, http://www.sigmaaldrich.com) prepared to 20 ppm in dichloromethane (Lab-Scan, http://www.labscan.ie/)).

The stir bar was thermally desorbed into the thermal desorption unit using the following desorption temperature program: initial temperature of 40°C, ramping at 100°C per min until 150°C, and a holding time of 5 min. The transfer temperature was 300°C, working in splitless desorption mode. The volatiles thermally desorbed were cryo-focused in the cooled injector system inlet at −100°C using liquid nitrogen, with a carrier gas flow of 50 ml min^{-1}. After cryo-focusing was completed, the volatiles were transferred into the capillary column by heating the CIS4 inlet at a rate of 10°C sec^{-1} to 150°C (holding time 3 min).

Mass spectra were collected in the scan range *m/z* 30–450. The measurements were performed using an electron bombardment ion source with electron energy of 70 eV. The transfer line, source and quadrupole temperatures were set at 280, 230 and 150°C, respectively. The chromatograms and mass spectra were evaluated using ChemStation software (G1791CA, version D.03.00; Agilent Technologies). Chromatographic peak identification was performed by library matching using the Standard Reference Database 1A NIST 2005, version 2.0 (National Institute of Standards and Technology, http://www.nist.gov/rsd/nist1a.cfm).

Quantitative PCR

Total RNA was isolated from 100 mg homogenized plant material using an RNeasy mini kit (Qiagen, http://www.qiagen.com/default.aspx), including DNase treatment. cDNA was synthesized from 1 μg total RNA using a Maxima® first strand cDNA synthesis kit (Fermentas, http://www.fermentas.com/en/home).

Quantitative RT-PCR reactions were performed using SYBR Premix ExTaq™ (Takara, http://www.takara-bio.com/) on a Rotor-Gene Q machine (Qiagen). The housekeeping gene *ubiquitin protein ligase* was used for relative quantification of gene expression. In order to minimize the variability, we used three biological replicates and two technical replicates for each sample. We obtained take-offs and efficiency values and computed differences in gene expression analysis as described previously and using the REST program (Pfaffl *et al.*, 2002; Delgado-Benarroch *et al.*, 2009a; Mallona *et al.*, 2010, 2011).

Antirrhinum transformation

We developed a new protocol to obtain stable transformants (Appendix S1). These transformants were further analyzed by PCR using primers for the *NPTII* gene. Two independent plants positive for *NPTII* that showed phenotypes that ranged from the classic null allele def^{gli} to weak alleles such as def^{nic} were also used.

Statistics

Statistical analysis was performed using the R package (www.r-project.org/) and Excel (Microsoft, www.microsoft.com). Unless otherwise stated, we used the Kruskal–Wallis test because growth and cellular data were not normally distributed.

Graphical modelling

The graphic models describing the currently known and proposed transcriptional networks were programmed in the Dot graph specification language and visualized using Graphviz (http://www.graphviz.org).

ACKNOWLEDGEMENTS

This work was funded by the Ministerio de Ciencia e Innovación/Fondos Europeos de Desarrollo Regional, FEDER (project BFU-2010-15843). We would like to thank Dr Leandro Peña (Centro de Protección Vegetal y Biotecnología, Instituto Valenciano de Investigaciones Agrarias, Valencia, Spain) for suggesting the use of *Agrobacterium tumefaciens* strains for transformation. We are grateful to Dr Barry Causier (Institute of Integrative and Comparative Biology, Faculty of Biological Sciences University of Leeds, UK) and Fabiola Ruiz Ramón for comments on the manuscript.

SUPPORTING INFORMATION

Additional Supporting Information may be found in the online version of this article:

Figure S1. Segregation of colour in F_2 of the *co* mutant.

Figure S2. GC-MS profiles of volatiles.

Figure S3. Phenotypes of the additional weak *RNAi-DEF* line.

Table S1. Primers for quantitative RT-PCR and cloning.

Appendix S1. Detailed *Antirrhinum majus* transformation protocol.

Please Note: As a service to our authors and readers, this journal provides supporting information supplied by the authors. Such materials are peer-reviewed and may be re-organized for online delivery, but are not copy-edited or typeset. Technical support issues arising from supporting information (other than missing files) should be addressed to the authors.

REFERENCES

Almeida, J., Carpenter, R., Robbins, T.P., Martin, C. and Coen, E.S. (1989) Genetic interactions underlying flower color patterns in *Antirrhinum majus*. *Genes Dev.* **3**, 1758–1767.

Alon, U. (2007) Network motifs: theory and experimental approaches. *Nat. Rev. Genet.* **8**, 450–461.

Anastasiou, E. and Lenhard, M. (2007) Growing up to one's standard. *Curr. Opin. Plant Biol.* **10**, 63–69.

Angenent, G.C., Franken, J., Busscher, M., Colombo, L. and van Tunen, A.J. (1993) Petal and stamen formation in petunia is regulated by the homeotic gene *fbp1*. *Plant J.* **4**, 101–112.

Baumann, K., Perez-Rodriguez, M., Bradley, D., Venail, J., Bailey, P., Jin, H.L., Koes, R., Roberts, K. and Martin, C. (2007) Control of cell and petal morphogenesis by R2R3 MYB transcription factors. *Development*, **134**, 1691–1701.

Bayo-Canha, A., Delgado-Benarroch, L., Weiss, J. and Egea-Cortines, M. (2007) Artificial decrease of leaf area affects inflorescence quality but not floral size in *Antirrhinum majus*. *Sci. Hortic.* **113**, 383–386.

Berbel, A., Navarro, C., Ferrandiz, C., Canas, L.A., Beltran, J.P. and Madueno, F. (2005) Functional conservation of PISTILLATA activity in a pea homolog lacking the PI motif. *Plant Physiol.* **139**, 174–185.

Bey, M., Stuber, K., Fellenberg, K., Schwarz-Sommera, Z., Sommer, H., Saedler, H. and Zachgo, S. (2004) Characterization of Antirrhinum petal

development and identification of target genes of the class B MADS box gene *DEFICIENS*. *Plant Cell*, **16**, 3197–3215.

Bradley, D., Carpenter, R., Sommer, H., Hartley, N. and Coen, E. (1993) Complementary floral homeotic phenotypes result from opposite orientations of a transposon at the *plena* locus of antirrhinum. *Cell*, **72**, 85–95.

Carpenter, R. and Coen, E.S. (1990) Floral homeotic mutations produced by transposon mutagenesis in *Antirrhinum majus*. *Genes Dev.* **4**, 1483–1493.

Cartolano, M., Efremova, N., Kuckenberg, M., Raman, S. and Schwarz-Sommer, Z. (2009) Enhanced *AGAMOUS* expression in the centre of the Arabidopsis flower causes ectopic expression over its outer expression boundaries. *Planta*, **230**, 857–862.

Causier, B., Bradley, D., Cook, H. and Davies, B. (2009) Conserved intragenic elements were critical for the evolution of the floral C-function. *Plant J.* **58**, 41–52.

Causier, B., Schwarz-Sommer, Z. and Davies, B. (2010) Floral organ identity: 20 years of ABCs. *Semin. Cell Dev. Biol.* **21**, 73–79.

Coen, E.S. and Meyerowitz, E.M. (1991) The war of the whorls: genetic interactions controlling flower development. *Nature*, **353**, 31–37.

Das, P., Ito, T., Wellmer, F., Vernoux, T., Dedieu, A., Traas, J. and Meyerowitz, E.M. (2009) Floral stem cell termination involves the direct regulation of AGAMOUS by PERIANTHIA. *Development*, **136**, 1605–1611.

Davies, B., DiRosa, A., Eneva, T., Saedler, H. and Sommer, H. (1996a) Alteration of tobacco floral organ identity by expression of combinations of Antirrhinum MADS-box genes. *Plant J.* **10**, 663–677.

Davies, B., Egea-Cortines, M., de Andrade, S.E., Saedler, H. and Sommer, H. (1996b) Multiple interactions amongst floral homeotic MADS box proteins. *EMBO J.* **15**, 4330–4343.

Davies, B., Motte, P., Keck, E., Saedler, H., Sommer, H. and Schwarz-Sommer, Z. (1999) PLENA and FARINELLI: redundancy and regulatory interactions between two Antirrhinum MADS-box factors controlling flower development. *EMBO J.* **18**, 4023–4034.

Delgado-Benarroch, L., Causier, B., Weiss, J. and Egea-Cortines, M. (2009a) FORMOSA controls cell division and expansion during floral development in *Antirrhinum majus*. *Planta*, **229**, 1219–1229.

Delgado-Benarroch, L., Weiss, J. and Egea-Cortines, M. (2009b) The mutants *compacta ähnlich*, *Nitida* and *Grandiflora* define developmental compartments and a compensation mechanism in floral development in *Antirrhinum majus*. *J. Plant. Res.* **122**, 559–569.

Di Stilio, V.S., Martin, C., Schulfer, A.F. and Connelly, C.F. (2009) An ortholog of *MIXTA-like2* controls epidermal cell shape in flowers of *Thalictrum*. *New Phytol.* **183**, 718–728.

Dornelas, M.C., Patreze, C.M., Angenent, G.C. and Immink, R.G.H. (2011) MADS: the missing link between identity and growth? *Trends Plant Sci.* **16**, 89–97.

Dudareva, N., Murfitt, L.M., Mann, C.J., Gorenstein, N., Kolosova, N., Kish, C.M., Bonham, C. and Wood, K. (2000) Developmental regulation of methyl benzoate biosynthesis and emission in snapdragon flowers. *Plant Cell*, **12**, 949–961.

Dudareva, N., Martin, D., Kish, C.M., Kolosova, N., Gorenstein, N., Faldt, J., Miller, B. and Bohlmann, J. (2003) (*E*)-β-ocimene and myrcene synthase genes of floral scent biosynthesis in snapdragon: function and expression of three terpene synthase genes of a new terpene synthase subfamily. *Plant Cell*, **15**, 1227–1241.

Egea Gutierrez-Cortines, M. and Davies, B. (2000) Beyond the ABCs: ternary complex formation in the control of floral organ identity. *Trends Plant Sci.* **5**, 473–478.

Egea-Cortines, M., Saedler, H. and Sommer, H. (1999) Ternary complex formation between the MADS-box proteins SQUAMOSA, DEFICIENS and GLOBOSA is involved in the control of floral architecture in *Antirrhinum majus*. *EMBO J.* **18**, 5370–5379.

Espinosa-Soto, C., Padilla-Longoria, P. and Alvarez-Buylla, E.R. (2004) A gene regulatory network model for cell-fate determination during *Arabidopsis thaliana* flower development that is robust and recovers experimental gene expression profiles. *Plant Cell*, **16**, 2923–2939.

Ferrandiz, C., Gu, Q., Martienssen, R. and Yanofsky, M.F. (2000) Redundant regulation of meristem identity and plant architecture by *FRUITFULL*, *APETALA1* and *CAULIFLOWER*. *Development*, **127**, 725–734.

Fujiwara, T., O'Geen, H., Keles, S., Blahnik, K., Linnemann, A.K., Kang, Y.A., Choi, K., Farnham, P.J. and Bresnick, E.H. (2009) Discovering hematopoietic mechanisms through genome-wide analysis of GATA factor chromatin occupancy. *Mol. Cell*, **36**, 667–681.

Geuten, K., Viaene, T. and Irish, V.F. (2011) Robustness and evolvability in the B-system of flower development. *Ann. Bot.* **107**, 1545–1556.

Goodwin, S., Kolosova, N., Kish, C.M., Wood, K.V., Dudareva, N. and Jenks, M.A. (2003) Cuticle characteristics and volatile emissions of petals in *Antirrhinum majus*. *Physiol. Plant.* **117**, 435–443. Erratum in *Physiol. Plant.* **119**, 605.

Halfter, U., Ali, N., Stockhaus, J., Ren, L. and Chua, N.H. (1994) Ectopic expression of a single homeotic gene, the *Petunia* gene *green petal*, is sufficient to convert sepals to petaloid organs. *EMBO J.* **13**, 1443–1449.

Heintzen, C., Nater, M., Apel, K. and Staiger, D. (1997) AtGRP7, a nuclear RNA-binding protein as a component of a circadian-regulated negative feedback loop in *Arabidopsis thaliana*. *Proc. Natl Acad. Sci. USA*, **94**, 8515–8520.

Helliwell, C. and Waterhouse, P. (2003) Constructs and methods for high-throughput gene silencing in plants. *Methods*, **30**, 289–295.

Honma, T. and Goto, K. (2000) The Arabidopsis floral homeotic gene *PISTILLATA* is regulated by discrete *cis*-elements responsive to induction and maintenance signals. *Development*, **127**, 2021–2030.

Irish, V.F. and Yamamoto, Y.T. (1995) Conservation of floral homeotic gene function between Arabidopsis and Antirrhinum. *Plant Cell*, **7**, 1635–1644.

Jackson, D., Roberts, K. and Martin, C. (1992) Temporal and spatial control of expression of anthocyanin biosynthetic genes in developing flowers of *Antirrhinum majus*. *Plant J.* **2**, 425–434.

Kalir, S., Mangan, S. and Alon, U. (2005) A coherent feed-forward loop with a SUM input function prolongs flagella expression. *Escherichia coli. Mol. Syst. Biol.* **1**, 2005.0006.

Kaufmann, K., Muino, J.M., Jauregui, R., Airoldi, C.A., Smaczniak, C., Krajewski, P. and Angenent, G.C. (2009) Target genes of the MADS transcription factor SEPALLATA3: integration of developmental and hormonal pathways in the *Arabidopsis* flower. *PLoS Biol.* **7**, 854–875.

Kaufmann, K., Nagasaki, M. and Jauregui, R. (2010a) Modelling the molecular interactions in the flower developmental network of *Arabidopsis thaliana*. *In Silico Biol.* **10**, 125–143.

Kaufmann, K., Wellmer, F., Muino, J.M. *et al.* (2010b) Orchestration of floral initiation by APETALA1. *Science*, **328**, 85–89.

Kempin, S.A., Savidge, B. and Yanofsky, M.F. (1995) Molecular basis of the cauliflower phenotype in Arabidopsis. *Science*, **267**, 522–525.

Kolosova, N., Sherman, D., Karlson, D. and Dudareva, N. (2001) Cellular and subcellular localization of *S*-adenosyl-L-methionine: benzoic acid carboxyl methyltransferase, the enzyme responsible for biosynthesis of the volatile ester methylbenzoate in snapdragon flowers. *Plant Physiol.* **126**, 956–964.

Krizek, B.A. and Meyerowitz, E.M. (1996) The Arabidopsis homeotic genes *APETALA3* and *PISTILLATA* are sufficient to provide the B class organ identity function. *Development*, **122**, 11–22.

Kuckuck, H. and Schick, R. (1930) Die Erbfaktoren bei *Antirrhinum majus* und ihre Bezeichnung. *Z. Indukt. Abstamm. Vererbungsl.* **56**, 51–83.

Laitinen, R.A.E., Pollanen, E., Teeri, T.H., Elomaa, P. and Kotilainen, M. (2007) Transcriptional analysis of petal organogenesis in *Gerbera hybrida*. *Planta*, **226**, 347–360.

Lenser, T., Theissen, G. and Dittrich, P. (2009) Developmental robustness by obligate interaction of class B floral homeotic genes and proteins. *PLoS Comput. Biol.* **5**, e1000264.

Ma, W., Lai, L., Ouyang, Q. and Tang, C. (2006) Robustness and modular design of the *Drosophila* segment polarity network. *Mol. Syst. Biol.* **2**, 70.

Maier, A.T., Stehling-Sun, S., Wollmann, H., Demar, M., Hong, R.L., Haubeiss, S., Weigel, D. and Lohmann, J.U. (2009) Dual roles of the bZIP transcription factor PERIANTHIA in the control of floral architecture and homeotic gene expression. *Development*, **136**, 1613–1620.

Mallona, I., Lischewsky, S., Weiss, J., Hause, B. and Egea-Cortines, M. (2010) Validation of endogenous genes as controls for quantitative real-time PCR during leaf and flower development in *Petunia hybrida*. *BMC Plant Biol.* **10**, 4.

Mallona, I., Weiss, J. and Egea-Cortines, M. (2011) PcrEfficiency: a web tool for PCR amplification efficiency calculus. *BMC Bioinformatics*, **12**, 404.

Martin, C. and Gerats, T. (1993) Control of pigment biosynthesis genes during petal development. *Plant Cell*, **5**, 1253–1264.

Martin, C., Prescott, A., Mackay, S., Bartlett, J. and Vrijlandt, E. (1991) Control of anthocyanin biosynthesis in flowers of *Antirrhinum majus*. *Plant J.* **1**, 37–49.

Melzer, R. and Theissen, G. (2009) Reconstitution of floral quartets *in vitro* involving class B and class E floral homeotic proteins. *Nucleic Acids Res.* **37**, 2723–2736.

Noda, K., Glover, B.J., Linstead, P. and Martin, C. (1994) Flower colour intensity depends on specialized cell shape controlled by a Myb-related transcription factor. *Nature*, **369**, 661–664.

Pelaz, S., Ditta, G.S., Baumann, E., Wisman, E. and Yanofsky, M.F. (2000) B and C floral organ identity functions require *SEPALLATA* MADS-box genes. *Nature*, **405**, 200–203.

Perez-Rodriguez, M., Jaffe, F.W., Butelli, E., Glover, B.J. and Martin, C. (2005) Development of three different cell types is associated with the activity of a specific MYB transcription factor in the ventral petal of *Antirrhinum majus* flowers. *Development*, **132**, 359–370.

Pfaffl, M.W., Horgan, G.W. and Dempfle, L. (2002) Relative expression software tool (REST©) for group-wise comparison and statistical analysis of relative expression results in real-time PCR. *Nucleic Acids Res.* **30**, e36.

Pnueli, L., Hareven, D., Broday, L., Hurwitz, C. and Lifschitz, E. (1994) The *Tm5* MADS box gene mediates organ differentiation in the three inner whorls of tomato flowers. *Plant Cell*, **6**, 175–186.

Reale, L., Porceddu, A., Lanfaloni, L., Moretti, C., Zenoni, S., Pezzotti, M., Romano, B. and Ferranti, F. (2002) Patterns of cell division and expansion in developing petals of *Petunia hybrida*. *Sex. Plant Reprod.* **15**, 123–132.

Rijpkema, A.S., Royaert, S., Zethof, J., van der Weerden, G., Gerats, T. and Vandenbussche, M. (2006) Analysis of the *Petunia TM6* MADS box gene reveals functional divergence within the DEF/AP3 lineage. *Plant Cell*, **18**, 1819–1832.

Schwanhäusser, B., Busse, D., Li, N., Dittmar, G., Schuchhardt, J., Wolf, J., Chen, W. and Selbach, M. (2011) Global quantification of mammalian gene expression control. *Nature*, **473**, 337–342.

Schwarz-Sommer, Z., Huijser, P., Nacken, W., Saedler, H. and Sommer, H. (1990) Genetic control of flower development by homeotic genes in *Antirrhinum majus*. *Science*, **250**, 931–936.

Schwarz-Sommer, Z., Hue, I., Huijser, P., Flor, P.J., Hansen, R., Tetens, F., Lonnig, W.E., Saedler, H. and Sommer, H. (1992) Characterization of the Antirrhinum floral homeotic MADS-box gene *deficiens* – evidence for DNA-binding and autoregulation of its persistent expression throughout flower development. *EMBO J.* **11**, 251–263.

Schwarz-Sommer, Z., Gubitz, T., Weiss, J., Gomez-di-Marco, P., Delgado-Benarroch, L., Hudson, A. and Egea-Cortines, M. (2010) A molecular recombination map of *Antirrhinum majus*. *BMC Plant Biol.* **10**, 275.

Sieburth, L.E., Running, M.P. and Meyerowitz, E.M. (1995) Genetic separation of third and fourth whorl functions of AGAMOUS. *Plant Cell*, **7**, 1249–1258.

Smaczniak, C., Immink, R.G.H., Muino, J.M. *et al.* (2012) Characterization of MADS-domain transcription factor complexes in Arabidopsis flower development. *Proc. Natl Acad. Sci. USA*, **109**, 1560–1565.

Sommer, H., Beltran, J.P., Huijser, P., Pape, H., Lonnig, W.E., Saedler, H. and Schwarz-Sommer, Z. (1990) *Deficiens*, a homeotic gene involved in the control of flower morphogenesis in *Antirrhinum majus*: the protein shows homology to transcription factors. *EMBO J.* **9**, 605–613.

Stubbe, H. (1966) *Genetik und Zytologie von Antirrhinum L. sect. Antirrhinum*. Germany: Veb Gustav Fischer Verlag, Jena.

Szecsi, J., Joly, C., Bordji, K., Varaud, E., Cock, J.M., Dumas, C. and Bendahmane, M. (2006) BIGPETALp, a bHLH transcription factor is involved in the control of Arabidopsis petal size. *EMBO J.* **25**, 3912–3920.

Theissen, G. and Saedler, H. (2001) Plant biology – floral quartets. *Nature*, **409**, 469–471.

Trobner, W., Ramirez, L., Motte, P., Hue, I., Huijser, P., Lonnig, W.E., Saedler, H., Sommer, H. and Schwarz-Sommer, Z. (1992) *GLOBOSA*: a homeotic gene which interacts with *DEFICIENS* in the control of *Antirrhinum* floral organogenesis. *EMBO J.* **11**, 4693–4704.

Vainstein, A., Lewinsohn, E., Pichersky, E. and Weiss, D. (2001) Floral fragrance. New inroads into an old commodity. *Plant Physiol.* **127**, 1383–1389.

Vandenbussche, M., Zethof, J., Souer, E., Koes, R., Tornielli, G.B., Pezzotti, M., Ferrario, S., Angenent, G.C. and Gerats, T. (2003) Toward the analysis of the petunia MADS box gene family by reverse and forward transposon insertion mutagenesis approaches: B, C, and D floral organ identity functions require *SEPALLATA*-like MADS box genes in petunia. *Plant Cell*, **15**, 2680–2693.

Vandenbussche, M., Zethof, J., Royaert, S., Weterings, K. and Gerats, T. (2004) The duplicated B-class heterodimer model: whorl-specific effects and complex genetic interactions in *Petunia hybrida* flower development. *Plant Cell*, **16**, 741–754.

Varghese, J. and Cohen, S.M. (2007) microRNA miR-14 acts to modulate a positive autoregulatory loop controlling steroid hormone signaling in *Drosophila*. *Genes Dev.* **21**, 2277–2282.

Vincent, C.A. and Coen, E.S. (2004) A temporal and morphological framework for flower development in *Antirrhinum majus*. *Can. J. Bot.* **82**, 681–690.

Wang, Y.Q., Melzer, R. and Theissen, G. (2010) Molecular interactions of orthologues of floral homeotic proteins from the gymnosperm *Gnetum gnemon* provide a clue to the evolutionary origin of 'floral quartets'. *Plant J.* **64**, 177–190.

Weiss, D., Vanderluit, A.H., Kroon, J.T.M., Mol, J.N.M. and Kooter, J.M. (1993) The Petunia homolog of the *Antirrhinum majus candi* and *Zea mays A2* flavonoid genes; homology to flavanone 3-hydroxylase and ethylene-forming enzyme. *Plant Mol. Biol.* **22**, 893–897.

Whitney, H.M., Chittka, L., Bruce, T.J. and Glover, B.J. (2009a) Conical epidermal cells allow bees to grip flowers and increase foraging efficiency. *Curr. Biol.* **19**, 948–953.

Whitney, H.M., Kolle, M., Andrew, P., Chittka, L., Steiner, U. and Glover, B.J. (2009b) Floral iridescence, produced by diffractive optics, acts as a cue for animal pollinators. *Science*, **323**, 130–133.

Whitney, H.M., Poetes, R., Steiner, U., Chittka, L. and Glover, B.J. (2011) Determining the contribution of epidermal cell shape to petal wettability using isogenic Antirrhinum lines. *PLoS One*, **6**, e17576.

Winter, K.U., Weiser, C., Kaufmann, K., Bohne, A., Kirchner, C., Kanno, A., Saedler, H. and Theissen, G. (2002) Evolution of class B floral homeotic proteins: obligate heterodimerization originated from homodimerization. *Mol. Biol. Evol.* **19**, 587–596.

Yu, H., Ito, T., Zhao, Y., Peng, J., Kumar, P. and Meyerowitz, E.M. (2004) Floral homeotic genes are targets of gibberellin signaling in flower development. *Proc. Natl Acad. Sci. USA*, **101**, 7827–7832.

Zachgo, S., Silva, E., Motte, P., Trobner, W., Saedler, H. and Schwarz-Sommer, Z. (1995) Functional analysis of the Antirrhinum floral homeotic *DEFICIENS* gene *in vivo* and *in vitro* by using a temperature-sensitive mutant. *Development*, **121**, 2861–2875.